International Journal of E-Health and Medical Communications
Volume 14 • Issue 1

Detection of Antibiotic Constituent in *Aspergillus flavus* Using Quantum Convolutional Neural Network

Sannidhan M. S., NMAM Institute of Technology (deemed), India*
Jason Elroy Martis, NMAM Institute of Technology (deemed), India
Ramesh Sunder Nayak, Canara Engineering College, India
Sunil Kumar Aithal, NMAM Institute of Technology (deemed), India
Sudeepa K. B., NMAM Institute of Technology (deemed), India

ABSTRACT

Treatment of influenza and its complications is a major challenge for healthcare systems. Pyrazine is one drug used in treating influenza. Aspergillic acid is major antibiotic constituent in pyrazine compounds mined from *Aspergillus flavus*' final stage. This stage of flavus is detected through color change forming a pale-yellow crystal structure. Detection of the same is complex and demands an experienced fraternity to continuously monitor the growth of fungus and identify its color change. However, researches proved that the task needs to be perfect and a tiny human error leads to a catastrophe in antibiotic creation. To avoid these flaws, druggists make a huge investment on costly equipment for accurate detection. To overcome these drawbacks, this article proposes a hybrid quantum convolutional neural network that predicts various stages of the fungus from the microscope's sample. To train the network, about 47,000 samples were poised under typical lab settings. The proposed system was tested in usual conditions and positively isolated the mature samples with 96% efficiency.

KEYWORDS

Adaptive Denoising Filter, Antibacterial, Aspergillic Acid, *Aspergillus flavus*, Biomedicine, Quantum Convolutional Neural Networks, Quantum Variational Circuit, Transfer Learning

INTRODUCTION

Influenza is one of the lethal epidemics in the history of mankind and its variant human influenza A virus was discovered way back in the year 1933. Subsequently with its invention, health care management systems are continually thriving to combat it with enormous evolutions and gigantic efforts leading to different kinds of developments in the field of medicine. One such development

DOI: 10.4018/IJEHMC.321150 *Corresponding Author

concentrated in the area of molecular biology that lead to the invention of an anti influenza drug called pyrazine in the year 1980. However, with the adaptations to the conditions, the growth of virus kept mutating leading to several secondary infections in human beings out of which pneumonia is a well recorded one (Adalja et al., 2011). These complications further raise several challenges to health organizations and pharmaceutical organization to undergo continuous research and development in production of anti-bacterial drug to battle against them. Molecules bearing pyrazine moiety play important roles in pharmaceutical industry and have shown interesting antibacterial activities. Pyrazine nucleus have shown numerous pharmaceutical effects and one among them is fungal antibiotic (Aspergillic acid) (Wang et al., 2020). Based on spreading rate of Influenza, it is very crucial to also vary the dosage of antibiotics for effective treatment and manage their complications. Hence, it is very important for health management systems to electronically track the variations in the spread of disease and also to effectively communicate with pharmaceutical organizations. These dosages can be varied at the source of antibiotic production (Aspergillic acid) in the case of Aspergillus flavus' maturity cycle.

Aspergillus flavus is a commonly occurring fungus that is uniformly distributed across the entire planet. It forms to be one of the abundant and the wildly living fungus which all plants and animals depend upon. Being saprotrophic and pathogenic in nature, it acts as a primary reason for root rot in many legumes and other fruit bearing variety of plants. The genus flavus indicates the fungus is yellow in nature possessing yellowish tanned spores for growth. The toxin in these fungi can cause aspergillosis for immunocompromised humans. Aspergillus Flavus fulfills its entire life cycle in three main stages that last from fifteen to seventeen days. The primary stage is a spore launch stage of the fungus where it forms a greenish that last about five days. The secondary stage is the growing stage where the fungus establishes dominance over the growth medium which lasts to about five to six days. The final stage is the maturity stage in which the fungus nearly completes its life cycle and makes itself ready for the next generation by spreading spores around its vicinity. The first two stages are non-toxic to humans whereas the third stage can cause minor side effects to normal individuals. The last stage of the fungus is of keen interest among scientists due to the structure of the fungi. During this stage the fungus produces an acidic structure that increases the pH of the growing area thereby eliminating other co-existing lifeforms (Bhatnagar et al., 2014; Samanta et al., 2020).

In the year 1943, two eminent scientists White and Hill successfully revealed the origin of a substance within aspergillus flavus known as Aspergillic acid in the last stage of its life maturity. An aspergillus flavus altogether comprises of three stages out of which the third stage is considered as final stage of its maturity. The first stage of fungus is immature and comprises of only light green patches. Whereas the second stage of the fungus is hydrophilic in nature producing minor spores which enters the third stage only after five days. By its characteristics first and second stage is not significant for extracting any medicinal constituents. However, Aspergillic acid is produced only on reaching the third stage of maturity by passing the first and second stage completely. Aspergillic acid is organic in nature possessing bactericidal properties that aid in the development of antibiotics. Aspergillic acid is economical to extract when the fungus reaches its final maturity stage and the acid is completely neutral with no side effects to human beings due to its anti-carcinogenic property. Since Aspergillic acid is only produced during the final stages of the fungus' lifecycle it is extremely difficult to predict the stage of acid formation. It can be predicted only by experienced lab technicians who continuously monitor the fungus' growth in its medium. Traditionally this process was performed by adding the sample in the growth medium and continuously stirring the medium for uniform growth. The growing stage is monitored under a neutral light source for pale yellow crystalline structure. However, the technique seemed to be highly cumbersome as it involved high level of expertise in the area and is also prone to human errors in analyzing the color differences. Since color difference was the primary method for deducing the mature stage, with the increasing advancements in color image processing techniques some computerized techniques were deduced to ease the manual process. Most popular among them was Histogram analysis which observed complete changes for color modes in

the solution. Unfortunately, the method did not perform well because pale yellow was very faint for normal camera. As a solution to the prevailing drawback of the earlier technique, improvement was done by enhancing the quality of camera which further increased product extraction costs making identification costlier than the extraction itself (Sehgal et al., 2019; Amin et al., 2020).

To overcome the fallacies encountered due to the existing approaches, we have devised a deep learning solution by using a hybrid Quantum Convolutional Neural Network (QCNN) of 14,000 neurons on an average (Abbas et al., 2021; Schuld and Petruccione, 2018; Dunjko and Briegel, 2018). The process involved stripping out unwanted trained layers and tinkering necessary neurons and quantum qubits to benefit our objective of detecting the final maturity stage of fungus. These networks were meticulously trained with around 47,000 samples to overcome all best- and worst-case circumstances. The first level of training achieved a lower accuracy rate of 82% due to inefficient pre-processing algorithms at the source camera leading to the utilization of poor-quality images for training. In order to overcome these issues, we modified the existing QCNN by incorporating a custom pre-processor algorithm based on adaptive denoising filter to compensate the ill effects of the camera microscopy thereby enhancing and speeding up the training process with the images of higher quality (Mei et al., 2022; Fernandes et al., 2019; Acharya et al., 2019). By this we could enhance the stage detection process thereby increasing the overall training and evaluation process of our proposed system. The advised approach could achieve an overall accuracy rate of more than 96% which is by far a remarkable standard for Aspergillus flavus' stage detection uncovering the easy extraction of Aspergillic acid.

To design the proposed system, the research article has following key contributions:

- Creation of dataset with labelled fungal samples classified amongst three categories: Initial, Maturity and Extraction.
- Implementation of a Deep Neural Network to isolate the final stage of fungus.
- Application of an enhanced quantum variational circuit to increase the performance of fungal stage classification.
- Design of a hybrid architecture to amalgamate Classical Neural Network and a quantum variational circuit.

RELATED WORK

A research work conducted by Chavan et al. (2015) discussed the importance of pyrazine in treating influenza and its post complications. Experimental outcomes presented in the article proved the reduction in complications by more than 70%. Another article published by Khambholja and Asudani (2020) presented various details on post COVID complications leading to influenza and conducted good number of experimental investigations using pyrazine drug with varying doses to treat the complications. Outcomes of their experimentations prove the effect of varying the dosages to treat influenza and also achieved success rate of 85%. Few researches enlightened the importance of Aspergillic acid in the production of pyrazine drug. One such review article published by Chisca et al. (2016) exposed importance of Aspergillic acid which is a large antibiotic component in pyrazine. Outcomes of review proved the ability of aspergillus flavus and its maturity stage in producing Aspergillic acid. Wang et al. (2020) further conducted chemical investigation of fungus related to aspergillus flavus. From their investigations, they discovered the pyrazine-based derivatives largely accommodated in Aspergillic acid.

Malysheva et al. (2014) in their research exertion proved that aspergillus flavus is one of the highly significant classes of Aspergillus genus meant for producing one of the most relevant proteins that is required for the creation of secondary metabolites. In this article authors have extracted third stage of the flavus that is responsible for the delivery of required proteins causing able metabolism. In one of the research works accomplished by Chu et al. (2018) focused on the prediction of parasitic

and non-parasitic flavus based on spectroscopy images in connection to human beings. In their work, they have evidently classified the growth of the flavus into different stages and when it crosses the third stage of growth, the flavus turns out to be parasitic causing effects for human health. Gilbert et al. (2018) conducted research to classify S-strain and L-strain type flavus for the purpose of identification of excessive aflatoxin. In their study, they witnessed that L-strain type of flavus have greater amount of aflatoxin and the ingesting of any crop infected by the same would cause threats to the human health. From their work, it was evidently noted that the color composition of L-strain flavus occurring in the later stage is darker than the color of S-strain flavus. Another research article published by Mamo et al. (2017) also conducted research on detecting the classes of flavus to detect the containment of aflatoxin. In this research, authors have utilized a color agent over the sample of flavus and based on color composition, they were able to identify flavus with enormous aflatoxin. Investigating the outcomes of the work, it is observed that addition of color agent to the darker sample instigates higher amount of color which is classified as positive for aflatoxin containment.

Martis and Balasubramani (2020) proposed the utilization of Noiseless silhouettes by fusion filters in their work to extract the postural features efficiently. In their work they have used Kinect device to obtain a depth map of the input image. Obtained image contained noises which were denoised by the noiseless silhouettes. Results obtained were promising and aided for the greater rate of accuracy for detecting the body postures. Aspandi et al. (2021) proposed technique of incorporating fusion filters denoising technique inside the recurrent neural networks. The filter overcomes distortion in the facial landmarks and enhanced performance was observed when applied to facial analysis applications. In the research article articulated by Singh et al. (2018) incorporated noiseless silhouettes as a pre-processor for the purpose detecting the objects via CNN within the noisy images. The proposed technique utilized the incorporation of fusion filters within the CNN to train the denoised images and the comparative outcomes depicted in the paper achieved higher rate of accuracy for the CNN with denoising filter.

Mital et al. (2020) proposed a work that aimed at the automated classification of different categories of fungi that could replace the traditional tedious manual approach of using microscope. Authors in their proposed approach adopted the usage of pre-trained deep learning models to classify fungal images into 9 different classes corresponding to their variants. Study achieved a better accuracy of more than 93%. Article published by Zhou et al. (2019) proposed a system that can identify the fungal spores within the sample of human sputum. Authors incorporated the pre-trained convolution neural networks that could identify the classes of fungal spores within the sputum. However, the work could not achieve a higher rate of accuracy which is below 70%. Arredondo-Santoyo et al. (2019), in their research article conducted work on the classification of different fungal strains based on dye decolourisation using automated transfer learning models. They have also compared their proposed system with the machine learning models and achieved a higher classification rate of 95% for the transfer learning which is 20% higher than the machine learning models. In their research article Hur et al. (2022) proposed a QCNN model with two qubits for the purpose of classifying the classical data. They have further performed the comparative analysis of different QCNN models that are structurally different from each other in terms of encoding and other cost parameters. The experimental outcomes achieved from their work proved the better ability of QCNN models under different circumstances with the same level of training. Another work carried out by Henderson et al. (2020) utilized a transformation layer for CNN powered by random quantum circuits meant for image recognition. Experimental investigation was conducted using classical MNIST dataset housing more than seventy thousand images. On having a very closer look at the outcomes achieved, they evidently proved that the CNN powered by quantum circuits boosted the classification accuracy by means of finer feature mapping technique. Jeswal et al. (2019) articulated a review paper exposing the study of different types of QCNN and the purposes used of the same for different types of applications. In their review paper they have discussed the concept of different quantum models emerging from the basic level and getting evolved to the higher potential. However, their analysis on experimental outcomes proved the ability of every quantum network in boosting the performance of existing artificial neural

networks in achieving higher accuracy with same level of training. A research article authored by Mari et al. (2020) extended the concept of transfer learning approach over a hybrid QCNN model to form a hybrid transfer learning model meant for image classification. Authors were successful in achieving hybrid QCNN model by connecting the traditional fully connected CNN model with a layer of quantum circuits that could perform the classification of features extracted via existing transfer learning models. From their experimental outcomes, researchers were successful in proving that the transfer learning approach performs better classification with higher accuracy on the hybrid QCNN when compared to any other classification approaches.

On conducting a detailed literature work by referring to standard research works carried out by eminent researchers, it is found out that a good number of research exertions focused on manual detection of flavus classes via usage of reagent samples and other chemical components. Very few research works based on deep learning and neural networks utilized fungal samples to detect certain types of diseases and abnormalities. However, none of the work focused on identification of maturity stages in fungal samples which is important for producing antibiotics via extraction of Aspergillic acid in the final stage of maturity. Further, extended research on QCNN models exposed the larger scope of gaining higher classification accuracies by fusing the classical CNN with QCNN models. The conclusion of the literature work stressed for the implementation of the proposed system using a hybrid QCNN model to classify maturity stages of fungal samples. Apart from these, the background investigations also exposed the contribution of Aspergillic acid extracted via aspergillus flavus in producing pyrazine drug which has a large impact in treating influenza and its related complications.

DATASET CREATION

Our dataset consists of multiple images of "Aspergillus Flavus" fungus that is taken from the sample automatically. The image is cleaned and denoised to obtain a clear concise image. In order to train our system to recognise the stages of this fungus, we must initially pass these sample images through a finite process. The process is explained below.

Invariant Rotation

Though the samples collected by our setup are denoised and cleaned, the samples are not in a standard format to train our neural network. To achieve this all images initially must appear in the same starting point. Else the deep learning system might misclassify the stages causing erroneous results (Alphonse et al., 2021). The rotation phase brings all images to begin in a single starting point. Equation (1) shows the indicative angle calculation.

$$\theta = tan^{-1}\left(\frac{\overline{y} - y_o}{\overline{x} - x_o}\right) \tag{1}$$

Here $\left(\overline{x}, \overline{y}\right)$ are the mean centroid points of the entire image. $\left(x_o, y_o\right)$ are the starting points of the image at the centre. θ forms to be the angle to be rotated counter clockwise. We perform rotation by calculating the fusion of the cosine and sine angle for the original points. Equation (2) and (3) presents the rotation formulae along x and y.

$$x_{new} = cos\theta * \left(x_{curr} - x_o\right) + sin\theta * \left(y_{curr} - y_o\right) \tag{2}$$

$$y_{new} = -sin\theta * \left(x_{curr} - x_o\right) + cos\theta * \left(y_{curr} - y_o\right) \tag{3}$$

Here $\left(x_{new}, y_{new}\right)$ are the new points of the image from current point $\left(x_{curr}, y_{curr}\right)$ rotated about the point $\left(x_0,\ y_0\right)$. We also have to take care of all unwanted pixels that do not associate with our image by using equation (4)

$$\left(x_{val}, y_{val}\right) = \begin{Bmatrix} x_{new}\ if W_{left} < x_{curr} > W_{right}, H_{left} < y_{curr} > H_{right} \\ \left(0,0\right)\ \ Otherwise \end{Bmatrix} \tag{4}$$

Here $\left(x_{val}, y_{val}\right)$ are the pixel values of the old image. W_{left}, W_{right} are the image width from the left and the right of the image centre. H_{left}, H_{right} are the height of the image from the centre of the sample image respectively.

Shearing

Once the image is invariantly rotated, we need to straighten the image in order to make the fungal spores appear round. This occurs due to a slight angle deviation that lies while taking the sample from the microscope. The angle deviation is shown in Figure 1. In the figure, original viewpoint refers to the sample taken at an exact vertical top view which is completely suitable for capturing the sample. Where as camera viewpoint represents the real time capture position.

The camera viewpoint needs to be corrected in order to get the original image. However, there are several unavoidable restrictions that arises when the camera is set to take the sample from the normal. A turnaround solution is to shear the image at a predestined angle from the original viewpoint (Zhou et al. 2021). Careful observation and experimental analysis found that the angle of deviation is six degrees. By examining the clarity of the capture at different angles on a trial and error basis, we have finalized six degrees as we have comparatively attained the best clarity. Utilizing this angle, we perform horizontal shearing to all images using the following equation (5).

$$\begin{aligned} x_{shear} &= x_{org} + \left(m * y_{org}\right) \\ y_{shear} &= y_{org} \end{aligned} \tag{5}$$

Figure 1.
Geometrical representation depicting the angle deviation from the normal

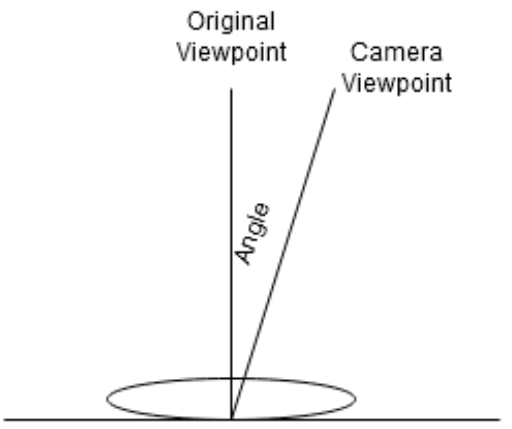

Here (x_{shear} , y_{shear}) are the shearing coordinate pixel values. The value m is calculated using tangent function of six degrees as shown in equation 6.

$$m = tan\theta \; where \; \theta = 6^{o} \tag{6}$$

Scaling

This step reduces the dimension of the image to a standard size for training. The larger the size of the image, the heavier the training time and increased memory size (Kim et al., 2022; Bello et al., 2021; Zhang et al., 2021). The standard prefixed size of choosing for images is $\left(224,224\right)$. The shearing formulae is shown equation (7).

$$\begin{aligned} H_{scaled} &= \left(H_{org} * 224\right) / W_{org} \\ W_{scaled} &= \left(W_{org} * 224\right) / H_{org} \end{aligned} \tag{7}$$

Here $\left(W_{org}, H_{org}\right)$ is the original height and width of the sample. $\left(W_{scaled}, H_{scaled}\right)$ is the scaled height and weight of the sample. In order to preserve sample consistency without losing data, we use interpolation operations along the height and width.

Dataset Agglomeration

Aspergillus Flavus passes through three stages from the initial to the maturity stage. This entire phase change takes around a total of sixty days. Meanwhile the fungus undergoes a lot of fine colour changes which makes the detection extremely difficult to handle. The setup shown in Figure 2 must also be kept in open sunlight since the fungus requires natural light to grow thus making sample extraction also difficult since sunlight varies. To avoid these issues a turnaround solution is to extract sample values at fixed intervals of five minutes in any lighting conditions which may lead to slight colour issues. The only issue lies with extracting three classes which is performed with the help of two human experts in the field of biotechnology.

Class Labelling

The class labeller process is used to extricate different stages of fungi for the sake of extraction. We perform this step as a helper for the future trainer. We perform this step manually to avoid any miscalculation for the training function (Kumar et al., 2021; Fernandes and Bala 2018). In addition to this it becomes very tedious to differentiate stages of fungal samples using automated approach. For our example, we have chosen only three stages, i.e., initial phase, maturity, and extraction phase.

There are clear distinguishable features in different stages of the fungus as shown in *Figure 2*. The initial Phase of Aspergillus has tiny spots scattered across the vial forming clumps. The colour of the solution is light green with darkish greenish green presence on the clumps. The Maturity phase of the fungus has a dark green presence which is completely filled on the entire vial. The sample has three distinguishable colour namely dark green which is prominent, light green clumps over the dark green and a brownish tinge on the sides of the vial. The extraction phase is when the fungus finishes its growth and is ready for extraction. The most prominent feature in this stage is light green structure with lines radiating from the centre resembling a cross section of a stem.

Since this dataset is not available anywhere, we need to create our own dataset of all samples distributes in a weighted ratio among the three different stages. The reason for choosing weighted ratio is to increase prediction accuracy at the extraction stage since this stage is our main target. We have set a fixed target ratio of 1:5:12.

Figure 2.
Fungal samples of different stages of *Aspergillus flavus*: (a) Initial stage, (b) growing stage, (c) maturity stage

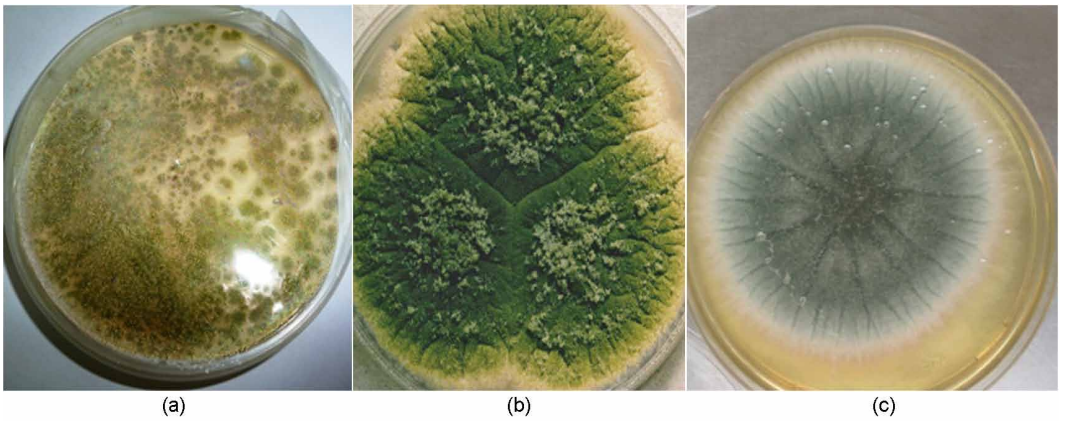

PROPOSED METHODOLOGY

Considering the drawbacks specified in the literature survey, in our methodology, we have proposed a simplified architecture as shown in Figure 3.

Our proposed system is divided into the six main stages: 1) Sample Capture, 2) Image Pre-processing, 3) Class Labelling, 4) Training via Quantum Convolutional Neural Network, 5) Validation and Testing, and 6) Prediction. Explanation corresponding to each stage is portrayed in detail in the following sub sections.

Sample Capture

This stage is the preliminary stage our system and is the most critical phase. The criticality factor arises because taking samples includes a laborious and tedious process. In order to minimize the labour and

Figure 3.
Architecture of our proposed system

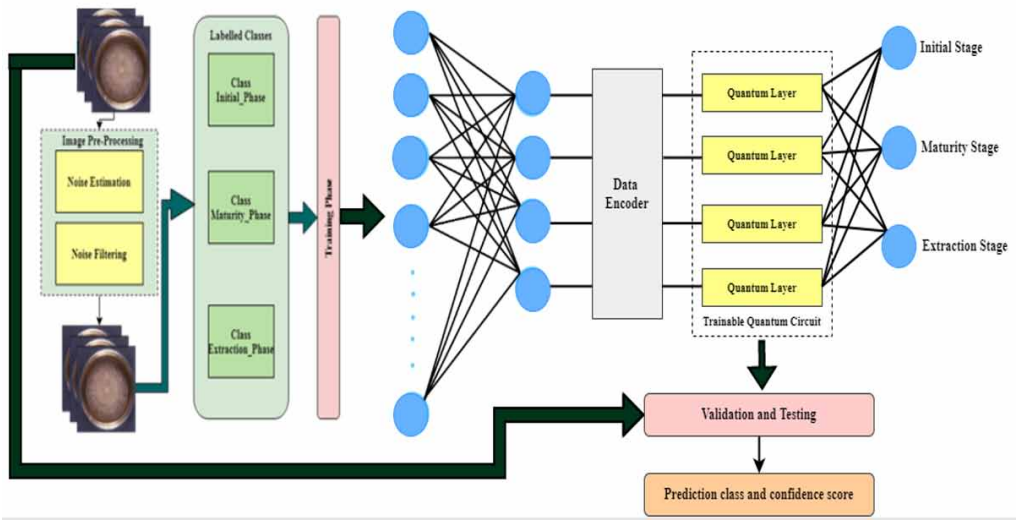

human error we automate the process by attaching an automated camera that taking sample images in fixed intervals. The setup of the automated sample collector is shown in Figure 4.

It is noteworthy to assume that the samples are not perfect and include a lot of noise and blurriness due to the camera's focus angle and CMOS sensor defects (Roth et al., 2022; Sugama et al., 2022; Chai and Choa, 2021). In addition to this there are lighting, and other conditions involved while taking samples since the fungus needs natural sunlight to grow. These vulnerabilities are treated in the next stage.

Image Pre-Processing

Here we take care of all vulnerabilities involved in the sample capture process. Our focus is to address two main issues that is noise estimation and noise filtering. We perform these steps to remove all strains of impulsive noise on the pixels of captured image produced due to minor defect in camera sensor. The strains of noises are classified as salt, pepper, and Poisson factored noises. We use an adaptable noise filtering function which takes care of denoising the pixels without blurring them and restoring their quality. Equation 8 shows the different noises and their denoising operations (Dong et al., 2022; Bharati et al., 2021; Anuradha et al., 2021; Fernandes et al., 2013).

$$I_d = I * P_I^g .where\, P_I^g = \begin{cases} \sqrt{1/2\pi\sigma} * e^{\frac{-(g-\mu)^2}{2\sigma^2}}, & if\, Gaussian\, Noises \\ I_a \quad ,if\, g = a\, Salt\, noises \\ I_b \quad ,if\, g = b\, Pepper\, noises \\ \frac{g^k ie^{-g}}{k!}, & if\, Poisson\, factored\, noises \end{cases} \tag{8}$$

Figure 4.
Overall setup of our automatic sample collector

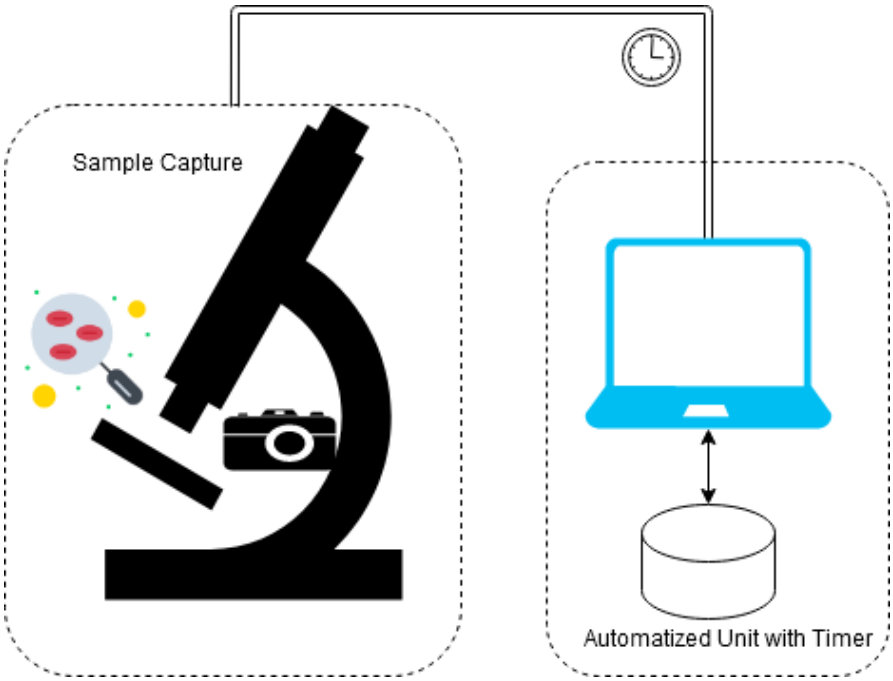

Here I_d, I denotes denoised images and original noisy images respectively. The factor functions within the braces are decided based on the probability distributed function P_I^g and pixel intensity value denoted by g. Our intention of using these fusion filters is to eliminate mixed noise types that exist in noisy images.

Training via Quantum Convolutional Neural Network

The training phase of our proposed system is the heart of our system. Here, we take annotated samples from the previous step and train our QCNN model to associate samples to any of the three classes. We have proposed the development of QCNN as a hybrid model with a combination of traditional neural network powered quantum computing (Sannidhan et al., 2021; Martis et al., 2020; Mittal et al., 2015; Sannidhan et al., 2019; Pallavi et al., 2021). Figure 5 shows our hybrid model architecture.

- **Classical Neural Network**

Our classical neural network module is used to extract feature vectors from the image datasets which are further utilized for the categorization into different labelled classes. In order to hasten the training time as well as increase extraction accuracy, we have adopted a pretrained transfer learning models from the ImageNet suite. We have selected different pretrained models based on the suitability of the image domain. We have selected the following models for our comparison. They are VGG16, VGG19, ResNet50, Dense Net 169, Dense Net 201, Xception, InceptionV3 and Mobile Net (Ke et al., 2021; Morid et al., 2021; Amin et al., 2019). The feature summary of our chosen models is shown in *Table 1*.

- **Quantum Circuit**

Variational circuits are also called parameterised quantum circuits. They play a role in Quantum Computing akin to the role played by Neural Networks in Classical Computing. In this work, based on the complexity level, we have implemented a quantum variational circuit comprising of three qubits. A qubit also addressed as a quantum bit represents a binary (0/1) bit in the classical computing environment. The purpose of the qubit is mainly to measure the super position of the electron spin within the magnetic

Figure 5.
QCNN model for fungal classification

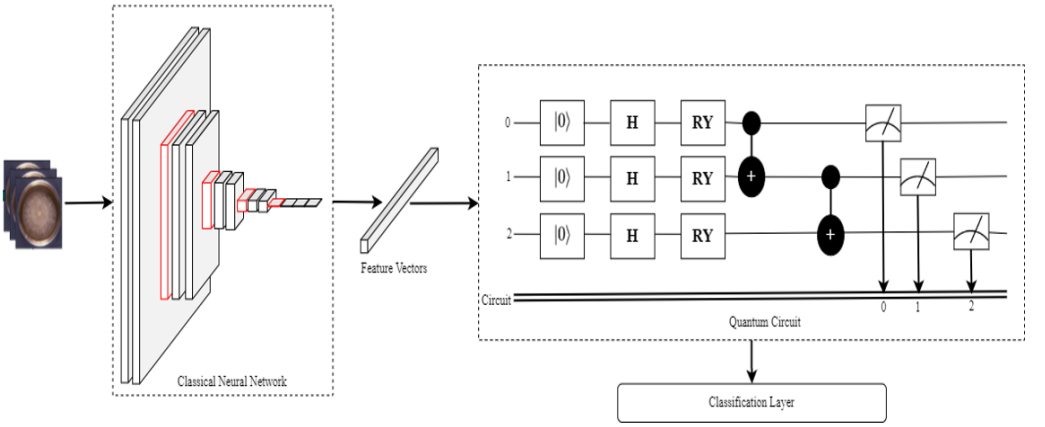

Table 1.
Architectural description of chosen transfer learning models

Model	Model Size	Total Convolutional Layers	Total Hyperparameters
VGG16	528MB	13	138,357,544
VGG19	549MB	16	143,667,240
ResNet50	99MB	53	25,636,712
Dense Net 169	57MB	150	14,307,880
Dense Net 201	80MB	219	20,242,984
Xception	88MB	36	22,910,480
InceptionV3	92MB	48	23,851,784
Mobile Net	17MB	13	4,253,864

field which is either spin-up (1) or a spin-down (0) state. Our quantum variational circuit comprises of following three important states namely Initial, Parameterized, and measurement state. The initial state is preliminary stage which resets all qubits to 0 which is denoted by $|0$. The parameterized quantum circuit consists of two parameters which are input and variational denoted by x and θ respectively. The mathematical denotation used to represent the quantum variation is $U\left(x,\theta\right)$ where U represents the function used to represent variation gates. Note that the inputs to these quantum circuits are performed using quantum embeddings which are classical data into quantum states using Hilbert's feature spaces. Figure 6 shows architecture of our chosen quantum circuit (Hou et al., 2022).

In Figure 6, R_x stands for the rotation operation in x axis which is represented by the matrix operation shown in equation (9)

$$R_x = exp\begin{pmatrix} \cos\frac{\theta}{2} & -i\sin\frac{\theta}{2} \\ -i\sin\frac{\theta}{2} & \cos\frac{\theta}{2} \end{pmatrix} \tag{9}$$

Here θ represents the rotation angle performed by the qubit. Similarly, U_3 represents a rotation amongst all three axes denoted by θ,ϕ,λ respectively. Its matrix representation is shown in equation (10)

Figure 6.
Proposed architecture of quantum variational circuit

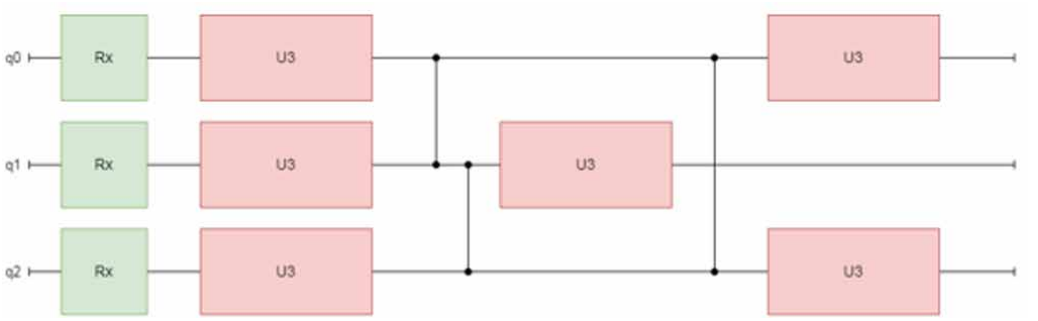

$$U_3\left(\theta,\phi,\lambda\right)=\begin{pmatrix}\cos\frac{\theta}{2} & -e^{i\lambda}\sin\frac{\theta}{2}\\ e^{i\phi}\sin\frac{\theta}{2} & e^{i\left(\phi+\lambda\right)}\cos\frac{\theta}{2}\end{pmatrix} \tag{10}$$

At the final stage, we perform measurement of our quantum states also called as expectation values. These expectation values can then be used by classical algorithms for post processing.

The equation (11) represents the mathematical formulation which describes the quantum embedding that translates extracted features into qubits.

$$|\,\delta := U_x\,|\,O^{\otimes D} \tag{11}$$

In the equation (10) δ represents the feature space extracted using classical neural networks which is encoded to D qubit Hilbert space. In our case the value of $D=3$. The quantum embedded feature space is then passed on to the variational circuit for quantum computations. The mathematical procedure of variational circuit is denoted in equation (12).

$$|\,g_\theta\left(x\right) := G_\theta\,|\,\Psi_x \tag{12}$$

In equation (11) G is a parameterized unitary evolving the state after the feature map to a new state, and the parameters $\theta\in\Theta$ are chosen to minimize a certain loss function.

Equation (13) fulfils the measurement component of the quantum circuit for post processing.

$$z=\left(z_1,z_2,z_3\right)\vDash f\left(z\right) \tag{13}$$

In Equation (13) z_1,z_2,z_3 represents the measured values from three qubits. $f\left(z\right)$ represents the model used to categorize the fungal samples.

- **Classification Layer**

The classification layer of our network is composed out of classical linear classifier which categorizes fungal samples into three different classes. The main purpose of using the classification layer is to imbibe simplicity and inversely transform the quantum computed values. Figure 7 presents the detailed architecture of our classification layers.

Our classification layer is divided into following four fully connected layers: 1) FC 1, 2) FC2, 3) FC3 and 4) FC4. Each fully connected layer FC1, FC2, FC3 and FC4 is a feed forward neural networks that receives the input from the final pooling layer in the form of a measure qubits. Each of the subsequent layer has a decreasing order of neurons to classify the features obtained via measured qubits. The detailed description of each of the layer is depicted in Table 2 (Amin et al. 2018).

QCNN Enhancement Algorithm

In this section, we have portrayed the pseudo-code depicting the implementation of our proposed system involving the enhancement of QCNN pre-processor using adaptive denoising filters. Entire pseudocode is structured sequentially to understand in a simple way.

Figure 7.
Classification layer architecture

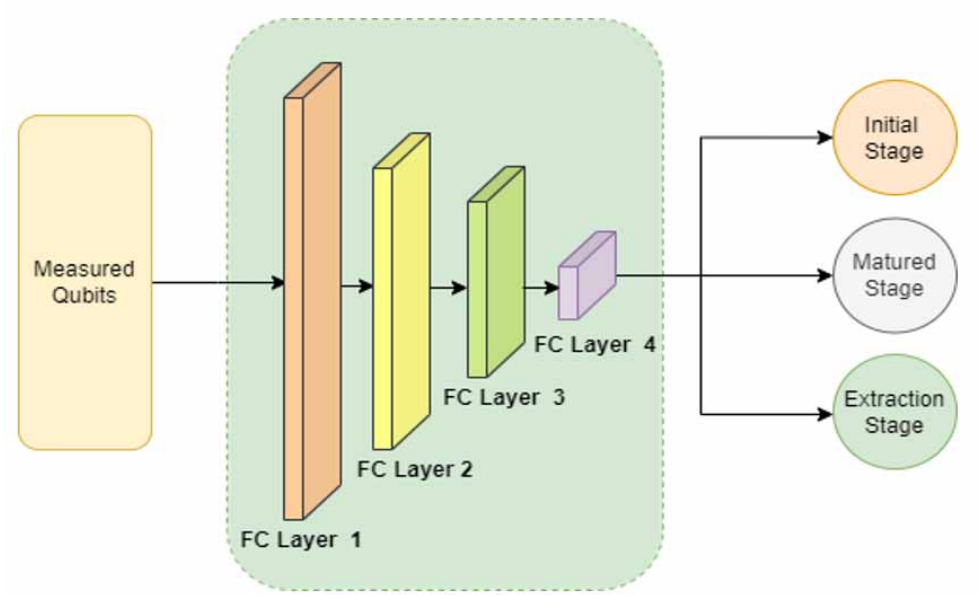

Table 2.
Classification layer parameters

Layer Name	Number of Neurons	Total Hyperparameters
FC1	100	400
FC2	50	5050
FC3	20	1020
FC4	3	63

Algorithm 1. Enhanced QCNN using Adaptive Denoising Filter.
Input: Image from camera
Output: Fungal stage (Initial, Maturity, Extraction)
for each pretrained classification model f, **do**
for n training samples, **do**
$I\left(x_{org}, y_{org}\right) \leftarrow$ Capture sample from camera in Pixel Format.
$\left(W_{org}, H_{org}\right) \leftarrow$ Length and Width of Image Format
$m \leftarrow \tan\left(6^{o}\right)$
$x_{shear} \leftarrow x_{org} + \left(m * y_{org}\right)$
$y_{shear} \leftarrow y_{org}$
$H_{scaled} = \left(H_{org} * 224\right) / W_{org}$
$W_{scaled} = \left(W_{org} * 224\right) / H_{org}$
$I_{d} \leftarrow I\left(x_{shear}, y_{shear}\right)$

11 $I \leftarrow I_d * P_I^g .where P_I^g = \left\{ \begin{array}{c} \sqrt{1/2\pi\sigma * e^{\frac{-(g-\mu)^2}{2\sigma^2}}}, \quad if\, Gaussian\, Noises \\ I_a \quad ,if\, g = a\, Salt\, noises \\ I_b \quad ,if\, g = b\, Pepper\, noises \\ \frac{g^k ie^{-g}}{k!}, \quad if\, Poisson\, factored\, noises \end{array} \right\}$

12 $Wts \leftarrow Initialize\, Random\, Weights$

13 **for** every batch of images, **do**

14 $(W, H) \leftarrow (W_{org}, H_{org})$

15 $L_{stages} \leftarrow \left\{ \begin{array}{c} Initial \\ Maturity \\ Extraction \end{array} \right\}$

16 $\partial(f_1) \leftarrow \left\{ \partial\left(Wts * \left[\frac{1}{1+e^{-f}}\right]\right) \Big/ \partial(L_{stages}) \right\}$

17 $\partial(f_2) \leftarrow \left(\frac{1}{1+e^{-f_1}}\right)$

18 $\forall q_n \leftarrow VQA(R_x, U_3)$

19 end for

20 $Map(I, L) \leftarrow \left\{ \partial(I * f_2) \Big/ \partial(f_2) \right\}$

21 end for

22 end for

The pseudocode presented in algorithm 1 represents the mathematical procedure of implementing our proposed QCNN model. The preliminary part of our proposed system involves the design of a preprocessor with adaptive denoising filter. Hence lines 3 to 11 depicts design of the preprocessor mathematically. Once after the design of preprocessor, the proposed system focused on stage categorization required for training. Line 15 implements the approach of labelling the classes of images. Line 16 to 18 portrays the design and training procedure of our hybrid QCNN model which is the last stage of our proposed system. This set of activities are performed iteratively for every chose classification model.

EXPERIMENTAL INVESTIGATION AND DISCUSSIONS

Our proposed system consists of three classes of the fungi "Aspergillus Flavus" having a total of about 17240 images in single trial classified around three categories. Among these the image distribution among the three classes are shown in Table 3. The reason of performing various trials is to prevent error rates in classifications that denotes the number of images in the dataset being corrupted in terms of its visual quality.

Visual Quality Assessment of the Dataset Samples

Since, we have applied a pre-processing operative in our system, we have tabulated the influence of pre-processing function that we have applied on our fungal samples with respect to our QCNN architectures. In order to evaluate the quality of image with/ without pre-processor, we have adopted three standard no

Table 3.
Image distribution among maturity classes

Stages	Ratio Division	No of Images	Error Rate	Total Trials	Total Images
Initial	1	957	0.3%	3	2,871
Maturity	5	4785	1%	2	9,570
Extraction	12	11,484	0.27%	3	34,452
Total Images (Entire Dataset)					46,893

reference image quality evaluators: 1) Naturalness Image Quality Evaluator (NIQE), 2) Perception based Image Quality Evaluator (PIQE) and 3) Blind/Reference less Image Spatial Quality Evaluator (BRISQUE). In the following sections, we have given a brief description in regard to the mentioned no reference image quality evaluators. (You and Korhonen, 2022; Leveque et al., 2021; Qi et al., 2021; Gueraichi and Serir, 2020; Kinoshita and Kiya, 2019; Courtney, 2021; Fu et al., 2021; Chan and Goldsmith, 2002).

- **Naturalness Image Quality Evaluator (NIQE)**

This no reference image quality evaluator that evaluates the naturalness factor of the image under test. The technique is a neural network-based evaluator which is pre-trained with the images of different quality standards and generates a score between the range 1 to 20. Lesser the score value, it indicates the higher naturalness factor in the image.

- **Perception based Image Quality Evaluator (PIQE)**

This is another technique based on deep learning systems used to calculate the image quality with out using any reference images for the evaluation. The evaluator evaluates quality of any image by returning the spatial quality score computed from the input image that is supplied. The spatial quality score indicates the perceptual quality of an image and less the score higher is the quality of the image. The score ranges between the scale of 0 to 100 with 0 being highly excellent and 100 being worst quality.

- **Blind/Reference less Image Spatial Quality Evaluator (BRISQUE)**

BRISQUE is also a non-referential image quality evaluator used to evaluate noise and distortion factors appearing in the image. BRISQUE evaluator is a deep learning network consisting of pre-trained images with range of noise and distorted factors. The network is sensitive to noise and distortions and is costumed to generate the score based on amount of noise and distortion factors. The score generated by the network ranges between 0 to 100 with lower score indicating higher quality with less noise and other distortions.

We have utilized the discussed no referential image quality evaluators and its influence is portrayed in Table 4.

We know that NIQE, BRISQUE and PIQE are no referential quality indicators for the image. The image has a good perceptual quality if they have lower values. It is evident from Table 4 that pre-processor operations mentioned in our proposed system does indeed increase the quality of the image.

Analysis of Classification Accuracy

We have tested our classification system on a dual card Tesla P100 1024 core CPU having 128GB RAM and having a maximum clocking speed of 4.5TFLOPS. The software framework build was

Table 4.
Image quality of QCNN architectures with and without pre-processing elements

No Referential Image Quality	Average	
	With Pre-Processor	Without Pre-Processor
NIQE↓	12.97	14.1635
BRISQUE↓	7.927	10.8546
PIQE↓	6.334	15.314

TensorFlow 2.2.4 with Keras along with Qiskit. Under this section, we have presented the classification accuracy of our proposed model with respect to different classification models adopted.

- **Analysis of Training Accuracy**

In this section, we have portrayed the training accuracy of the adopted classification models under different epoch levels. Based on the stability in the training rate, we chosen our architecture execution up to 600 epochs. Table 5 summarizes the rate of training achieved under different epochs for different classification models.

On analysing the data depicted in Table 5, it is evidently noted that the accuracy of VGG19 surpasses that of other pre-trained models with an accuracy of more than 96% for 600 epochs. Comparing the accuracies attained for every hundred epochs, the pre-trained models almost reaches the stability at around 500 epochs with not more than .05% improvement. Hence, we have halted the training for 600 epochs.

- **Analysis of Training loss Incurred**

In this section of the paper, we presented the analysis of training loss obtained under different epochs. A training loss represents the difference between the expected output and the actual output. This loss occurs, when the weights are improperly converged during training. Figure 8 shows a graphical plot of all loss values occurred during training, out of which VGG19 has the least epoch value due its high accuracy curve shown in Table 5. Also, the training reaches stability at 500 epochs

Table 5.
Epoch wise Training accuracy of QCNN classification models

Architecture Name	Epochs Accuracy↑					
	100	200	300	400	500	600
VGG16	78.34%	83.45%	86.56%	89.76%	92.35%	92.37%
VGG19	84.34%	87.45%	92.74%	94.86%	96.47%	96.52%
ResNet50	56.45%	68.12%	73.23%	79.56%	82.65%	82.65%
Dense Net 169	65.23%	75.43%	87.98%	93.39%	95.63%	95.64%
Dense Net 201	67.92%	74.32%	86.57%	91.75%	94.35%	94.39%
Xception	72.34%	77.55%	85.60%	83.70%	91.39%	91.40%
InceptionV3	79.42%	83.45%	85.43%	89.64%	93.23%	93.22%
Mobile Net	52.40%	60.40%	63.60%	68.70%	71.50%	72.15%

as weights converged to the maximum amount. It can be inferred that Mobile Net experiences high loss whereas VGG 19 records least loss percentage.

• Comparative Analysis of Pre-Processor Influence

We have also performed the comparative analysis of our proposed QCNN model with and without the influence of the pre-processor adaptive de-noising filter. The main objective of the comparison is to uphold the importance of pre-processor in classification. Table 6 depicts the analysis data.

From Table 6 it is perceived that the pretrained models motioned with our classifier does recognize classes better by applying pre-processor operation rather than non-pre-processing operations. Since classification is one of the important characteristics of our system. It becomes a necessity to plot

Figure 8.
Plot depicting the loss values of our classification models

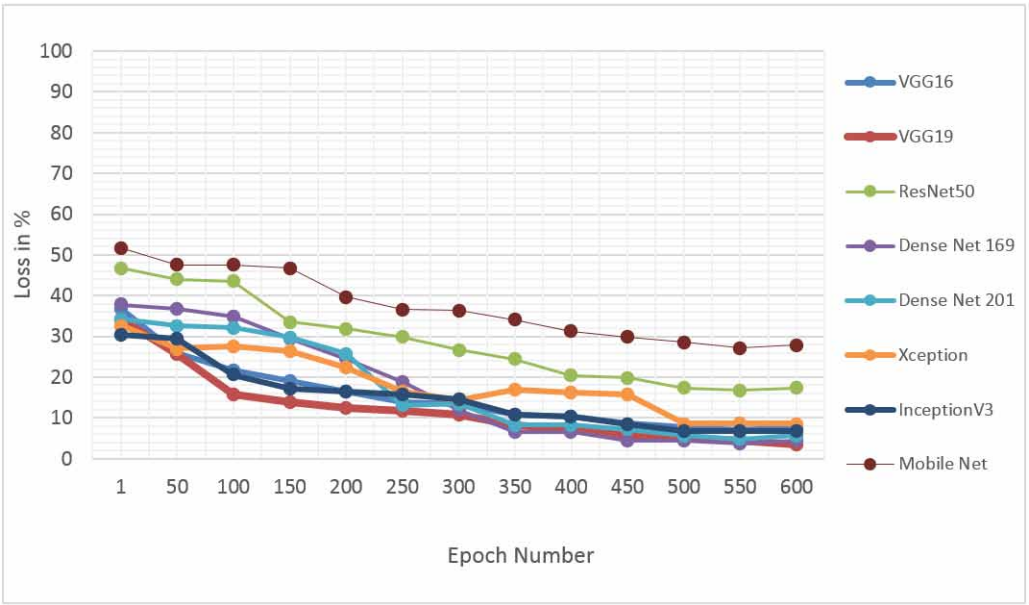

Table 6.
Accuracy analysis of QCNN with and without pre-processing

Model	Accuracy with Pre-Processor↑	Accuracy Without Pre-Processor↑
VGG16	92.37%	86.65%
VGG19	96.52%	82.47%
ResNet50	82.65%	78.6%
Dense Net 169	95.64%	86.34%
Dense Net 201	94.39%	87.56%
Xception	91.40%	86.49%
InceptionV3	93.22%	84.35%
Mobile Net	72.15%	63.48%

the confusion matrices of different models. Confusion matrix represents major tool for visualizing crucial data which facilitates to determine the classification errors generated by the various classifiers. Figure 9 shows the confusion matrices of all the selected models. Stages of "Aspergillus Flavus" is classified as initial, maturity and extraction categories in our work.

Observing the facts of confusion matrix presented in Figure 9, our system is successful in classifying the three phases of the "Aspergillus Flavus". It is also observed that we were successful in having higher accuracies to classify the extraction stage which is of utmost importance.

To analyze the overall strength classifying characteristics of our system, we have chosen Precision, Sensitivity, Specificity and F1-Score for our models. Table 7 shows the analysis of the chosen parameters.

It is apparent from Table 7 that VGG19 tops all other models by having better quantitative characteristics in classifying fungus' stages compared to other pretrained models. This is because of the number of hyperparameters as well as the increased number of convoluted layers in the model. Mobile Net receives the least score due to least number of misidentified classes.

- **Comparative Analysis of Proposed QCNN vs. Classical Neural Network**

Figure 9a.
(a)-(d) Confusion matrices for data portrayed in Table 6

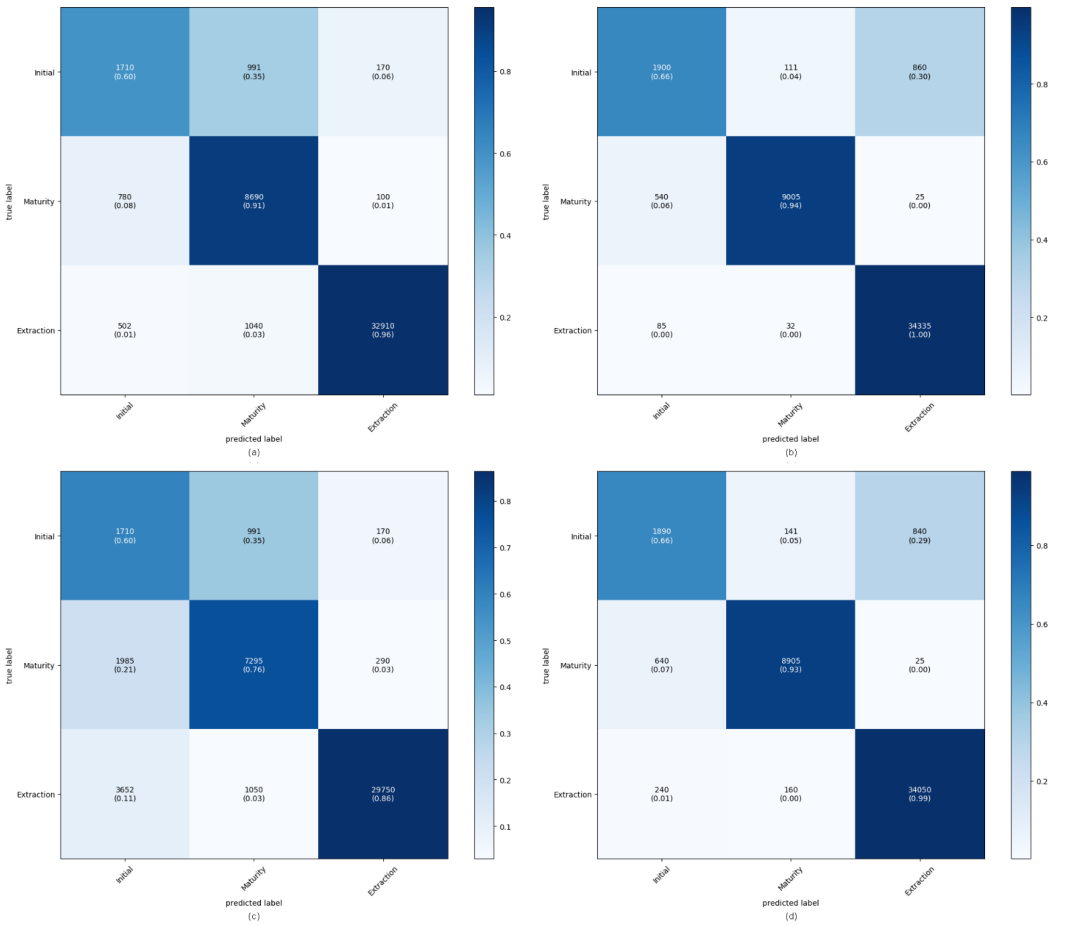

Figure 9b.
(e)-(h) Confusion matrices for data portrayed in Table 6

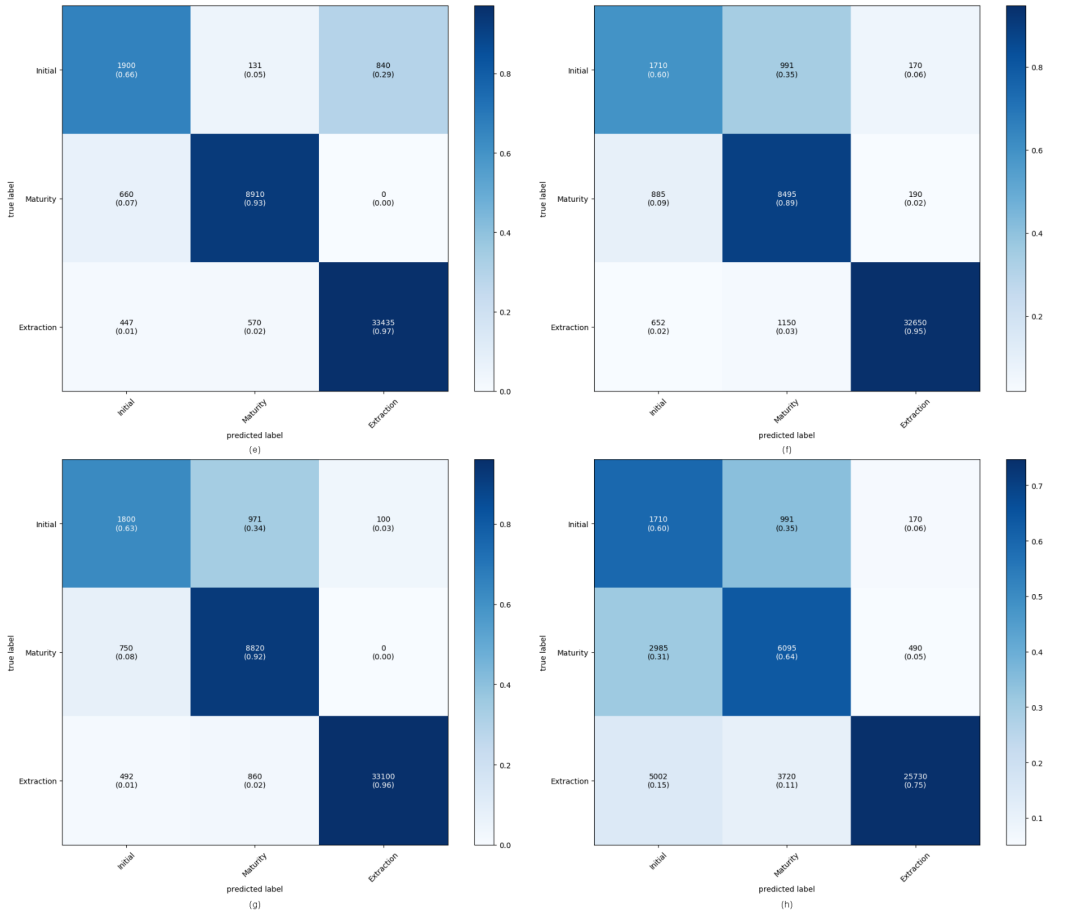

Table 7.
Statistical analysis of different QCNN architectures on various parameters

Model	VGG16	VGG19	ResNet50	Dense Net 169	Dense Net 201	Xception		Mobile Net
TP↑	44845	45240	44245	43720	43310	42855	38755	33535
TN↓	2046	1653	2648	3173	3583	4038	8138	13358
FP↑	91736	92133	91138	90613	90203	89748	85648	80428
FN↓	2046	1653	2648	3173	3583	4038	8138	13358
Precision (%) ↑	85.905	86.645	85.44333	83.645		81.03267	74.047	65.978
Recall (%) ↑			84.48033	80.56		77.14767	66.63	57.179
Specificity (%) ↑			0.471766			0.456945	0.413228	
F1 Score (%) ↑	0.95475		0.943531			0.913889	0.826456	

To further uphold the purpose of the utilization of QCNN, in this section, we have presented the comparative analysis of the classification accuracies with classical Neural Network. Table 8 presents the comparative analysis of classification accuracies of different models with QCNN and class Neural Network.

On performing the analysis of data presented in Table 8, it is strongly evident that the classification accuracy of all the adopted models are by far better when employed under QCNN compared to that of classical Neural Network. Figure 10 depicts the plot corresponding to the comparative analysis of the data portrayed in Table 8 for different classification models.

Observing the plot, it is very clearly noted that the accuracy of QCNN model is above the accuracy of classical Neural Network thus highlighting the importance of QCNN.

- **Comparative Analysis With State-of-the-Art Techniques**

We have also appraised the quality of our proposed system by comparing its accuracy with other state-of-the-art techniques from the well-known research works. Data presented in Table 9 portrays comparative analysis of the classification accuracy obtained from our proposed system with selected state-of-the-art techniques.

Table 8.
Comparative analysis of QCNN versus classical neural network

Model	QCNN↑	Classical Neural Network ↑
VGG16	92.37%	83.55%
VGG19	96.52%	78.34%
ResNet50	82.65%	69.65%
Dense Net 169	95.64%	82.61%
Dense Net 201	94.39%	79.56%
Xception	91.40%	81.38%
InceptionV3	93.22%	76.35%
Mobile Net	72.15%	56.48%

Figure 10.
Graphical analysis of QCNN with classical neural network

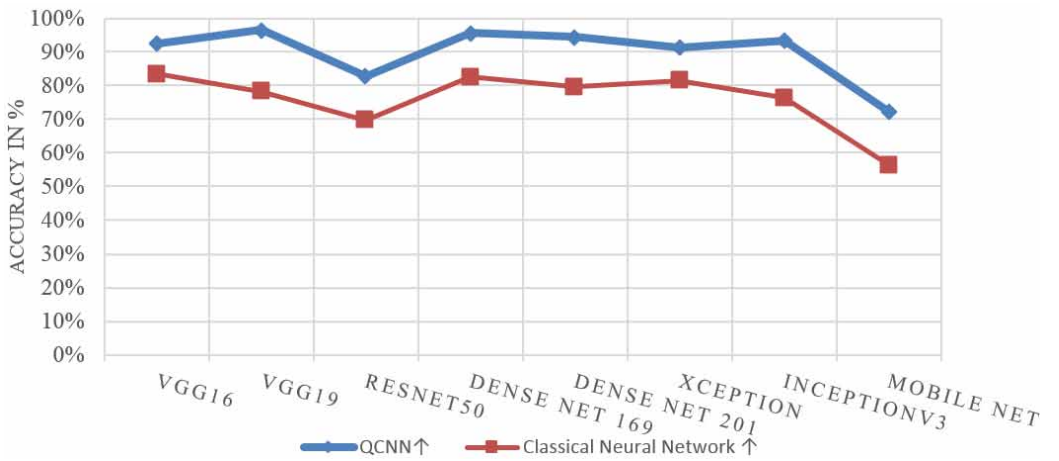

Table 9.
Proposed system accuracy comparison with other state-of-the-art techniques

Technique	Classification Accuracy
Siamese Network (Koch et al. 2015)	65%
Convolution Neural Network (Gaikwad et al. 2021)	69%
Deep-Ten (Zhang et al. 2017)	77%
Computer-assisted image processing (Korsnes et al. 2016)	71%
Proposed method with CNN	82%
Proposed method with QCNN	96%

By observing the data portrayed in Table 9, we can evidently prove that our proposed technique performs ably better when compared to other state-of-the-art techniques. Further it also upholds the importance of QCNN in enhancing the classification accuracy.

CONCLUSION

In this research exertion, we successfully accomplished the objective of detecting the final stage of maturity in Aspergillus Flavus via hybrid QCNN model. To further enhance the training efficiency, we have also modified the networks pre-processor layer by integrating an adaptive denoising filter that successfully eliminated all the different types of noises occurring in the fungal sample. Comparative analysis of outcomes proved that the modified QCNN performed higher than the classical Neural Network systems. To prove the ability of the pre-processor in enhancing the quality of image samples, we have also utilized standard no reference image evaluators. The maturity detection phase in our system helps in extracting varying amounts of pyrazine induced Aspergillic acid. Pyrazine drug has a greater impact in health management systems and pharmaceutical organizations dealing with complications related to influenza disease. Further, with the able electronic communication related to spread of influenza, the system can also be utilized to vary the dosage in the production stage itself.

In future, the work can be further extended to estimate the number of days required to reach maturity stage from initial stage. Apart from that there is a scope to denoise poor quality image samples using conditional generative adversarial networks having the ability to enhance an image captured even under low light conditions. Implementation of adversarial generative network would also aid in the development of artificial samples to enhance training process.

COMPETING INTERESTS

The authors of this publication declare there are no competing interests

FUNDING AGENCY

This research received no specific grant from any funding agency in the public, commercial, or not-for-profit sectors.

REFERENCES

Abbas, A., Sutter, D., Zoufal, C., Lucchi, A., Figalli, A., & Woerner, S. (2021). The power of quantum neural networks. *Nature Computational Science*, *1*(6), 403–409. doi:10.1038/s43588-021-00084-1

Acharya, U. R., Fernandes, S. L., WeiKoh, J. E., Ciaccio, E. J., Fabell, M. K. M., Tanik, U. J., Rajinikanth, V., & Yeong, C. H. (2019). Automated detection of Alzheimer's disease using brain MRI images–a study with various feature extraction techniques. *Journal of Medical Systems*, *43*(9), 1–14. doi:10.1007/s10916-019-1428-9 PMID:31396722

Adalja, A. A., Sappington, P. L., Harris, S. P., Rimmele, T., Kreit, J. W., Kellum, J. A., & Boujoukos, A. J. (2011). Isolation of Aspergillus in three 2009 H1N1 influenza patients. *Influenza and Other Respiratory Viruses*, *5*(4), 225–229. doi:10.1111/j.1750-2659.2011.00202.x PMID:21651732

Alphonse, A. S., Shankar, K., Jeyasheela Rakkini, M. J., Ananthakrishnan, S., Athisayamani, S., Robert Singh, A., & Gobi, R. (2021). A multi-scale and rotation-invariant phase pattern (MRIPP) and a stack of restricted Boltzmann machine (RBM) with preprocessing for facial expression classification. *Journal of Ambient Intelligence and Humanized Computing*, *12*(3), 3447–3463. doi:10.1007/s12652-020-02517-7

Amin, J., Sharif, M., Yasmin, M., & Fernandes, S. L. (2018). Big data analysis for brain tumor detection: Deep convolutional neural networks. *Future Generation Computer Systems*, *87*, 290–297. doi:10.1016/j.future.2018.04.065

Amin, J., Sharif, M., Yasmin, M., & Fernandes, S. L. (2020). A distinctive approach in brain tumor detection and classification using MRI. *Pattern Recognition Letters*, *139*, 118–127. doi:10.1016/j.patrec.2017.10.036

Amin, J., Sharif, M., Yasmin, M., Saba, T., Anjum, M. A., & Fernandes, S. L. (2019). A new approach for brain tumor segmentation and classification based on score level fusion using transfer learning. *Journal of Medical Systems*, *43*(11), 1–16. doi:10.1007/s10916-019-1453-8 PMID:31643004

Anuradha, P., Arabelli, R., & Rajkumar, K. (2021). Noise removal of ECG signals with adaptive filtering. *Materials Today: Proceedings*.

Arredondo-Santoyo, M., Domínguez, C., Heras, J., Mata, E., Pascual, V., Vázquez-Garcidueñas, M., & Vazquez-Marrufo, G. (2019). Automatic characterisation of dye decolourisation in fungal strains using expert, traditional, and deep features. *Soft Computing*, *23*(23), 12799–12812. doi:10.1007/s00500-019-03832-8

Aspandi, D., Martinez, O., Sukno, F., & Binefa, X. (2021). Composite recurrent network with internal denoising for facial alignment in still and video images in the wild. *Image and Vision Computing*, *111*, 104189. doi:10.1016/j.imavis.2021.104189

Bello, I., Fedus, W., Du, X., Cubuk, E. D., Srinivas, A., Lin, T. Y., & Zoph, B. et al. (2021). Revisiting resnets: Improved training and scaling strategies. *Advances in Neural Information Processing Systems*, *34*, 22614–22627.

Bharati, S., Khan, T. Z., Podder, P., & Hung, N. Q. (2021). A comparative analysis of image denoising problem: noise models, denoising filters and applications. In *Cognitive Internet of Medical Things for Smart Healthcare* (pp. 49–66). Springer. doi:10.1007/978-3-030-55833-8_3

Bhatnagar, D., Ehrlich, K. C., Moore, G. G., & Payne, G. A. (2014). Aspergillus Aspergillus flavus. Encyclopedia of food microbiology, 1, 83-91. doi:10.1016/B978-0-12-384730-0.00012-4

Chai, S. Y., & Choa, S. H. (2021). Reduction of Fluorine Diffusion and Improvement of Dark Current Using Carbon Implantation in CMOS Image Sensor. *Crystals*, *11*(9), 1106. doi:10.3390/cryst11091106

Chan, R. W. S., & Goldsmith, P. (2002). Modeling and validation of a psychovisually based image quality evaluator for DCT-based compression. *Signal Processing Image Communication*, *17*(6), 485–495. doi:10.1016/S0923-5965(02)00024-3

Chavan, R., Chaturvedi, P., & Chowdhary, A. (2015). Anti-influenza potential of alkaloidal molecules of jatropha curcas leaves. *International Journal of Pharmaceutical Sciences and Research*, *6*(11), 4705.

Chişca, D., Sterici, V., & Croitor, L. (2016). Mixed-ligand binuclear, 1D and 2D polymeric compounds of Cu (II), Zn (II) and Cd (II) with pyrazine carboxamide. In Materials Science and Condensed Matter Physics (pp. 135-135). Academic Press.

Chu, X., Wang, W., Ni, X., Zheng, H., Zhao, X., Zhang, R., & Li, Y. (2018). Growth Identification of Aspergillus flavus and Aspergillus parasiticus by visible/near-infrared hyperspectral imaging. *Applied Sciences (Basel, Switzerland)*, *8*(4), 513. doi:10.3390/app8040513

Courtney, J. (2021). SEDIQA: Sound Emitting Document Image Quality Assessment in a Reading Aid for the Visually Impaired. *Journal of Imaging*, *7*(9), 168. doi:10.3390/jimaging7090168 PMID:34460804

Dong, Y., Jiang, L., & Li, C. (2022). Improving data and model quality in crowdsourcing using co-training-based noise correction. *Information Sciences*, *583*, 174–188. doi:10.1016/j.ins.2021.11.021

Dunjko, V., & Briegel, H. J. (2018). Machine learning & artificial intelligence in the quantum domain: A review of recent progress. *Reports on Progress in Physics*, *81*(7), 074001. doi:10.1088/1361-6633/aab406 PMID:29504942

Fernandes, S. L., Bala, G. J., Nagabhushan, P., & Mandal, S. K. (2013, December). Robust Face Recognition in the presence of Noises and Blurring effects by fusing Appearance based techniques and Sparse Representation. In *2013 2nd International Conference on Advanced Computing, Networking and Security* (pp. 84-89). IEEE. doi:10.1109/ADCONS.2013.16

Fernandes, S. L., & Josemin Bala, G. (2018). Matching images captured from unmanned aerial vehicle. *International Journal of System Assurance Engineering and Management*, *9*(1), 26–32. doi:10.1007/s13198-016-0431-5

Fernandes, S. L., Rajinikanth, V., & Kadry, S. (2019). A hybrid framework to evaluate breast abnormality using infrared thermal images. *IEEE Consumer Electronics Magazine*, *8*(5), 31–36. doi:10.1109/MCE.2019.2923926

Fu, B., Spiller, N., Chen, C., & Damer, N. (2021, September). The effect of face morphing on face image quality. In *2021 International Conference of the Biometrics Special Interest Group (BIOSIG)* (pp. 1-5). IEEE. doi:10.1109/BIOSIG52210.2021.9548302

Gaikwad, S. S. (2021). Fungi classification using convolution neural network. *Turkish Journal of Computer and Mathematics Education*, *12*(10), 4563–4569.

Gilbert, M. K., Mack, B. M., Moore, G. G., Downey, D. L., Lebar, M. D., Joardar, V., Losada, L., Yu, J. J., Nierman, W. C., & Bhatnagar, D. (2018). Whole genome comparison of Aspergillus flavus L-morphotype strain NRRL 3357 (type) and S-morphotype strain AF70. *PLoS One*, *13*(7), e0199169. doi:10.1371/journal.pone.0199169 PMID:29966003

Gueraichi, R., & Serir, A. (2020, September). Blurred image detection in drone embedded system. In *2020 5th International Conference on Advanced Technologies for Signal and Image Processing (ATSIP)* (pp. 1-6). IEEE. doi:10.1109/ATSIP49331.2020.9231665

Henderson, M., Shakya, S., Pradhan, S., & Cook, T. (2020). Quanvolutional neural networks: Powering image recognition with quantum circuits. *Quantum Machine Intelligence*, *2*(1), 1–9. doi:10.1007/s42484-020-00012-y PMID:32879908

Hou, Y. Y., Li, J., Chen, X. B., & Ye, C. Q. (2022). A partial least squares regression model based on variational quantum algorithm. *Laser Physics Letters*, *19*(9), 095204. doi:10.1088/1612-202X/ac81b6

Hur, T., Kim, L., & Park, D. K. (2022). Quantum convolutional neural network for classical data classification. *Quantum Machine Intelligence*, *4*(1), 1–18. doi:10.1007/s42484-021-00061-x

Jeswal, S. K., & Chakraverty, S. (2019). Recent developments and applications in quantum neural network: A review. *Archives of Computational Methods in Engineering*, *26*(4), 793–807. doi:10.1007/s11831-018-9269-0

Ke, A., Ellsworth, W., Banerjee, O., Ng, A. Y., & Rajpurkar, P. (2021, April). CheXtransfer: performance and parameter efficiency of ImageNet models for chest X-Ray interpretation. In *Proceedings of the Conference on Health, Inference, and Learning* (pp. 116-124). doi:10.1145/3450439.3451867

Khambholja, K., & Asudani, D. (2020). Potential repurposing of Favipiravir in COVID-19 outbreak based on current evidence. *Travel Medicine and Infectious Disease*, *35*, 101710. doi:10.1016/j.tmaid.2020.101710 PMID:32360327

Kim, J. C., Le, D. T., Song, S. J., Son, C. H., & Choo, H. (2022, January). Multi-modal Fundus Image Registration with Deep Feature Matching and Image Scaling. In *2022 16th International Conference on Ubiquitous Information Management and Communication (IMCOM)* (pp. 1-3). IEEE. doi:10.1109/IMCOM53663.2022.9721768

Kinoshita, Y., & Kiya, H. (2019, September). Convolutional neural networks considering local and global features for image enhancement. In *2019 IEEE International Conference on Image Processing (ICIP)* (pp. 2110-2114). IEEE. doi:10.1109/ICIP.2019.8803194

Koch, G., Zemel, R., & Salakhutdinov, R. (2015, July). Siamese neural networks for one-shot image recognition. In ICML deep learning workshop (Vol. 2). Academic Press.

Korsnes, R., Westrum, K., Fløistad, E., & Klingen, I. (2016). Computer-assisted image processing to detect spores from the fungus Pandora neoaphidis. *MethodsX*, *3*, 231–241. doi:10.1016/j.mex.2016.03.011 PMID:27073786

Kumar, P., Ashtekar, S., Jayakrishna, S. S., Bharath, K. P., Vanathi, P. T., & Kumar, M. R. (2021, April). Classification of Mango Leaves Infected by Fungal Disease Anthracnose Using Deep Learning. In *2021 5th International Conference on Computing Methodologies and Communication (ICCMC)* (pp. 1723-1729). IEEE. doi:10.1109/ICCMC51019.2021.9418383

Lévêque, L., Outtas, M., Liu, H., & Zhang, L. (2021). Comparative study of the methodologies used for subjective medical image quality assessment. *Physics in Medicine and Biology*, *66*(15), 15TR02. doi:10.1088/1361-6560/ac1157 PMID:34225264

Malysheva, S. V., Arroyo-Manzanares, N., Cary, J. W., Ehrlich, K. C., Vanden Bussche, J., Vanhaecke, L., Bhatnagar, D., Di Mavungu, J. D., & De Saeger, S. (2014). Identification of novel metabolites from Aspergillus flavus by high resolution and multiple stage mass spectrometry. *Food Additives & Contaminants: Part A*, *31*(1), 111–120. doi:10.1080/19440049.2013.859743 PMID:24405210

Mamo, F. T., Selvaraj, J. N., Wang, Y., & Liu, Y. (2017). Recent developments in the screening of atoxigenic Aspergillus flavus towards aflatoxin biocontrol. *Journal of Applied & Environmental Microbiology*, *5*(1), 20–30.

Mari, A., Bromley, T. R., Izaac, J., Schuld, M., & Killoran, N. (2020). Transfer learning in hybrid classical-quantum neural networks. *Quantum*, *4*, 340. doi:10.22331/q-2020-10-09-340

Martis, J. E., & Balasubramani, R. (2020). Reckoning of emotions through recognition of posture features. *Journal of Applied Security Research*, *15*(2), 230–254. doi:10.1080/19361610.2019.1645530

Martis, J. E., Sudeepa, K. B., Sannidhan, M. S., & Bhandary, A. (2020, August). A rapid automated process for organizing bacterial cluster segments using deep neural networks. In *2020 Third International Conference on Smart Systems and Inventive Technology (ICSSIT)* (pp. 963-968). IEEE. doi:10.1109/ICSSIT48917.2020.9214173

Mei, S., Liu, M., Kudreyko, A., Cattani, P., Baikov, D., & Villecco, F. (2022). Bendlet Transform Based Adaptive Denoising Method for Microsection Images. *Entropy (Basel, Switzerland)*, *24*(7), 869. doi:10.3390/e24070869 PMID:35885092

Mital, M. E., Tobias, R. R., Villaruel, H., Maningo, J. M., Billones, R. K., Vicerra, R. R., ... Dadios, E. (2020, November). Transfer Learning Approach for the Classification of Conidial Fungi (Genus Aspergillus) Thru Pre-trained Deep Learning Models. In *2020 IEEE Region 10 Conference (TENCON)* (pp. 1069-1074). IEEE.

Mittal, P., Vatsa, M., & Singh, R. (2015, May). Composite sketch recognition via deep network-a transfer learning approach. In *2015 International Conference on Biometrics (ICB)* (pp. 251-256). IEEE. doi:10.1109/ICB.2015.7139092

Morid, M. A., Borjali, A., & Del Fiol, G. (2021). A scoping review of transfer learning research on medical image analysis using ImageNet. *Computers in Biology and Medicine*, *128*, 104115. doi:10.1016/j.compbiomed.2020.104115 PMID:33227578

Pallavi, S., Sannidhan, M. S., & Bhandary, A. (2021). Retrieval of facial sketches using linguistic descriptors: an approach based on hierarchical classification of facial attributes. In *Advances in Artificial Intelligence and Data Engineering* (pp. 1131–1149). Springer. doi:10.1007/978-981-15-3514-7_84

Qi, J., Deng, Y., Wang, Q., Yang, Z., Han, X., & Li, Y. (2021, October). Non-Reference Image Quality Assessment Based on Super-Pixel Segmentation and Information Entropy. In *2021 IEEE 9th International Conference on Computer Science and Network Technology (ICCSNT)* (pp. 110-114). IEEE. doi:10.1109/ICCSNT53786.2021.9615399

Roth, T., Tammes, S., Kaaret, P., DeRoo, C., & Packard, C. M. (2022). Characterization of gamma-ray-induced radiation effects on a commercial CMOS sensor for x-ray small satellites. *Journal of Astronomical Telescopes, Instruments, and Systems*, *8*(2), 026001. doi:10.1117/1.JATIS.8.2.026001

Samanta, A., Saha, A., Satapathy, S. C., Fernandes, S. L., & Zhang, Y. D. (2020). Automated detection of diabetic retinopathy using convolutional neural networks on a small dataset. *Pattern Recognition Letters*, *135*, 293–298. doi:10.1016/j.patrec.2020.04.026

Sannidhan, M. S., Prabhu, G. A., Chaitra, K. M., & Mohanty, J. R. (2021). Performance enhancement of generative adversarial network for photograph–sketch identification. *Soft Computing*, ●●●, 1–18.

Sannidhan, M. S., Prabhu, G. A., Robbins, D. E., & Shasky, C. (2019). Evaluating the performance of face sketch generation using generative adversarial networks. *Pattern Recognition Letters*, *128*, 452–458. doi:10.1016/j.patrec.2019.10.010

Schuld, M., & Petruccione, F. (2018). *Supervised learning with quantum computers* (Vol. 17). Springer. doi:10.1007/978-3-319-96424-9

Sehgal, I. S., Choudhary, H., Dhooria, S., Aggarwal, A. N., Bansal, S., Garg, M., Behera, D., Chakrabarti, A., & Agarwal, R. (2019). Prevalence of sensitization to Aspergillus flavus in patients with allergic bronchopulmonary aspergillosis. *Medical Mycology*, *57*(3), 270–276. doi:10.1093/mmy/myy012 PMID:29566248

Singh, M., Govil, M. C., & Pilli, E. S. (2018, October). V-SIN: Visual Saliency detection in noisy Images using convolutional neural Network. In *2018 Conference on Information and Communication Technology (CICT)* (pp. 1-6). IEEE. doi:10.1109/INFOCOMTECH.2018.8722431

Sugama, Y., Watanabe, Y., Kuroda, R., Yamamoto, M., Goto, T., Yasuda, T., Hamori, H., Kuriyama, N., & Sugawa, S. (2022). Two High-Precision Proximity Capacitance CMOS Image Sensors with Large Format and High Resolution. *Sensors (Basel)*, *22*(7), 2770. doi:10.3390/s22072770 PMID:35408384

Wang, F., Wei, M., Duan, X., Liu, X., Yao, S., Wang, J., Zhu, H., Chen, C., Gu, L., & Zhang, Y. (2020). Identification, synthesis and biological evaluation of pyrazine ring compounds from Talaromyces minioluteus (Penicillium minioluteum). *Organic Chemistry Frontiers : An International Journal of Organic Chemistry / Royal Society of Chemistry*, *7*(22), 3616–3624. doi:10.1039/D0QO01030H

You, J., & Korhonen, J. (2022). Attention integrated hierarchical networks for no-reference image quality assessment. *Journal of Visual Communication and Image Representation*, *82*, 103399. doi:10.1016/j.jvcir.2021.103399

Zhang, H., Xue, J., & Dana, K. (2017). Deep ten: Texture encoding network. In *Proceedings of the IEEE conference on computer vision and pattern recognition* (pp. 708-717). IEEE.

Zhang, Y., Li, K., Li, K., Sun, G., Kong, Y., & Fu, Y. (2021). Accurate and fast image denoising via attention guided scaling. *IEEE Transactions on Image Processing*, *30*, 6255–6265. doi:10.1109/TIP.2021.3093396 PMID:34242167

Zhou, Y., Feng, Y., & Zhang, H. (2019, April). Human Fungal Infection Image Classification Based on Convolutional Neural Network. In *Chinese Conference on Image and Graphics Technologies* (pp. 1-12). Springer. doi:10.1007/978-981-13-9917-6_1

Zhou, Y., Huang, H., Wang, H., Huang, Q., Song, T. S., & Xie, J. (2021). Efficient microbial electrosynthesis through the barrier and shearing effect of fillers. *International Journal of Hydrogen Energy*, *46*(73), 36103–36112. doi:10.1016/j.ijhydene.2021.08.129

Jason Elroy Martis is a dedicated Senior Assistant Professor in the Department of Information Science and Engineering at NMAM Institute of Technology, Nitte, Karnataka, India, where he has been serving since June 2009. In 2009, he earned his bachelor's degree in information science and engineering from Visvesvaraya Technological University, Belgaum. He then pursued a master's degree in computer science and engineering from the same university in 2013. In addition to his technical education, he also holds an MBA in marketing from KSOU, Mysore, Karnataka, India, which he completed between 2009 and 2011. With 14 years of teaching experience, Jason is a passionate teacher who has handled various subjects and research projects. His research interests include computer vision, image processing, artificial intelligence, deep learning and neural networks, cryptography, and information security. As a dedicated researcher with nine years of research experience, Jason has over 10 collaborative research publications, including journals, book chapters, and conference proceedings, in reputed indices. Apart from his academic work, Jason is also an active social worker and environmentalist. He serves as an honorary consultant to different agricultural industries to promote and sustain energy resources. He has been recognized by various organizations for his go-green initiative, where he runs his vehicle with eco-friendly Bio-Diesel. Jason's commitment to his work and passion for social and environmental causes make him an asset to any community.

Jason Elroy Martis is a dedicated Senior Assistant Professor in the Department of Information Science and Engineering at NMAM Institute of Technology, Nitte, Karnataka, India, where he has been serving since June 2009. In 2009, he earned his bachelor's degree in information science and engineering from Visvesvaraya Technological University, Belgaum. He then pursued a master's degree in computer science and engineering from the same university in 2013. In addition to his technical education, he also holds an MBA in marketing from KSOU, Mysore, Karnataka, India, which he completed between 2009 and 2011. With 14 years of teaching experience, Jason is a passionate teacher who has handled various subjects and research projects. His research interests include computer vision, image processing, artificial intelligence, deep learning and neural networks, cryptography, and information security. As a dedicated researcher with nine years of research experience, Jason has over 10 collaborative research publications, including journals, book chapters, and conference proceedings, in reputed indices. Apart from his academic work, Jason is also an active social worker and environmentalist. He serves as an honorary consultant to different agricultural industries to promote and sustain energy resources. He has been recognized by various organizations for his go-green initiative, where he runs his vehicle with eco-friendly Bio-Diesel. Jason's commitment to his work and passion for social and environmental causes make him an asset to any community.

Ramesh Sunder Nayak is working as Associate Professor in Canara Engineering College in IS&E Department. He has more than 20 years of experience. Reviewed many research papers. Area of interest: artificial intelligence, machine learning, image processing, big data, etc.

Sunil Kumar Aithal is an accomplished Assistant Professor in the Department of Computer Science and Engineering at NMAM Institute of Technology, situated in the beautiful region of Karnataka, India. He completed his bachelor's degree in information science in 2012 and his master's degree in computer science and engineering in 2014, both from VTU, Belagavi. Sunil's research interests encompass the areas of image processing, computer vision, and social analytics. His dedication to his field is reflected in the several research papers he has published in these areas, and he is currently pursuing his Ph.D. (part-time) at VTU, Belagavi, with immense enthusiasm. As a highly knowledgeable and committed educator, Sunil is an invaluable asset to his department and the academic community. His contributions to his field have helped shape the lives of many students and researchers, and his expertise continues to inspire future generations.

Sudeepa K. B. is currently working as associate professor for the Department of Computer Science, NMAMIT, Nitte, having 18 years of teaching experience and 9 years of research experience.